ISSN 1063-7745, Crystallography Reports, 2022, Vol. 67, No. 4, pp. 586–589. © Pleiades Publishing, Inc., 2022.
Russian Text © The Author(s), 2022, published in Kristallografiya, 2022, Vol. 67, No. 4, pp. 628–631.

STRUCTURE OF MACROMOLECULAR COMPOUNDS

Crystallization and Preliminary X-Ray Diffraction Analysis of Recombinant Phosphoribosylpyrophosphate Synthetase I from *Thermus thermophilus* HB27

Yu. A. Abramchik[a,b], V. I. Timofeev[a,b,c,], N. E. Zhukhlistova[b], M. B. Shevtsov[d], I. V. Fateev[a], M. A. Kostromina[a], E. A. Zayats[a], I. P. Kuranova[b,c,*], and R. S. Esipov[a]**

[a] *Shemyakin–Ovchinnikov Institute of Bioorganic Chemistry, Russian Academy of Sciences, Moscow, 117997 Russia*
[b] *Shubnikov Institute of Crystallography of Federal Scientific Research Centre "Crystallography and Photonics," Russian Academy of Sciences, Moscow, 119333 Russia*
[c] *National Research Centre "Kurchatov Institute," Moscow, 123098 Russia*
[d] *Moscow Institute of Physics and Technology, Dolgoprudnyi, Moscow oblast, 141701 Russia*
**e-mail: inna@ns.crys.ras.ru*
***e-mail: tostars@mail.ru*

Received November 22, 2021; revised December 1, 2021; accepted December 4, 2021

Abstract—Crystals of phosphoribosylpyrophosphate synthetase from the thermophilic bacterium *Thermus thermophilus* (Tth PRPPS1 HB27), suitable for X-ray diffraction, were grown by the hanging-drop vapor-diffusion method. Before X-ray diffraction data collection, the crystals were transferred to a cryoprotectant solution and were flash-frozen in liquid nitrogen stream. These crystals were used to collect the X-ray diffraction data set on the European Synchrotron Radiation Facility (ESRF, France, ID23-1 beamline) at 100 K to 2.6 Å resolution, which was suitable for determining the three-dimensional structure of the enzyme.

DOI: 10.1134/S1063774522040022

INTRODUCTION

Phosphoribosylpyrophosphate synthetases (PRPPSs, EC 2.7.6.1) are widespread in prokaryotic and eukaryotic organisms and are involved in essential biochemical processes, resulting in the biosynthesis of purine and pyrimidine bases [1, 2]. These enzymes catalyze the transfer of the β,γ-pyrophosphate group from adenosine triphosphate (ATP) to the glycosyl hydroxyl group of ribose 5-phosphate (Rib-5P), giving 5-phosphoribosylpyrophosphate (PRPP) and adenosine monophosphate (AMP) [3].

5-Phosphoribosylpyrophosphate, which is produced in the catalytic reaction, is an intermediate in the biosynthesis of purine and pyrimidine nucleotides, the amino acids histidine and tryptophan, and the NAD coenzyme [2]. PRPP is involved not only in the major (de novo) route but also in the salvage pathway of the biosynthesis of purine and pyrimidine nucleotides and acts as a regulator of both processes [4–6]. Therefore, PRPP belongs to metabolites that are constantly in demand by the cell and, consequently, PRPPS is a key enzyme important for the organism survival.

Phosphoribosylpyrophosphate synthetases are divided into three classes according to the quaternary structure, the mechanism of activity regulation, and the pyrophosphate-donor specificity [7–9]. There is the rather low sequence identity between three classes of PRPPSs. Class I PRPPSs includes a series of bacterial and mammalian enzymes, in particular, human PRPPS [10–12]. Class I enzymes have a high sequence homology [13]. The sequence identity between the *E. coli* and *B. subtilis* enzymes reaches 49.53% (84.76% homology); the identity between the *E. coli* and human PRPP synthetases is 47.50% (80.32% homology). Class I PRPPSs have a hexameric quaternary structure and strict selectivity for the pyrophosphate donor and the nature of the carbohydrate moiety. The activity of these enzymes depends on phosphate ions and is allosterically regulated through the binding of the ADP or guanosine diphosphate (GDP) molecule at the allosteric site. Only ATP is utilized as the pyrophosphate donor.

The three-dimensional structures of thermophilic PRPPSs have attracted interest due to the prospects of biotechnological applications of these enzymes. Previously, two phosphoribosylpyrophosphate synthetases, PRPPS1 and PRPPS2, encoded by the genes TT_C1184 and TT_C1274, respectively, were isolated from the thermophilic strain *Thermus thermophilus* HB27. Both enzymes belonging to class I differ in the sequence and some properties [14].

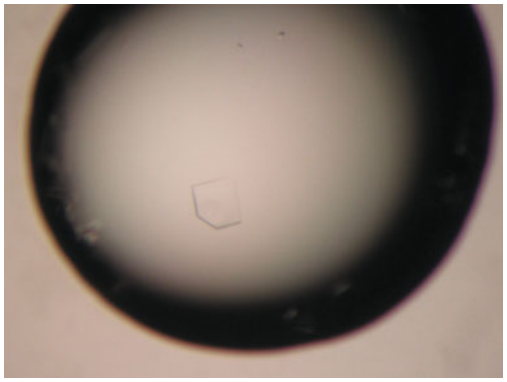

Fig. 1. Crystal of *Thermus thermophilus* phosphoribosylpyrophosphate synthetase Tth PRPPS1.

The three-dimensional structure of phosphoribosylpyrophosphate synthetase from the thermophilic bacterium *Thermus thermophilus* (Tth PRPPS2 HB27) was determined at 1.85 Å resolution (PDB_ID: 7AWO) from the X-ray diffraction data collected from rhombohedral crystals (sp. gr. *R*32), which were grown using lithium sulfate as a component of the reservoir solution [15], and at 2.2 Å resolution (PDB_ID: 5T3O) from the X-ray diffraction data measured from tetrahedral crystals (sp. gr. $P4_12_12$), which were grown using the reservoir solution containing ammonium sulfate [16].

Here we report the conditions of crystal growth for Tth PRPPS1 HB27. These crystals were used to collect the X-ray diffraction data to 2.6 Å resolution suitable for determining the three-dimensional structure of the enzyme.

MATERIALS AND METHODS

Phosphoribosylpyrophosphate synthetase from the thermophilic bacterium *Thermus thermophilus* (Tth PRPPS1 HB27) was produced as described in [14].

Table 1. X-ray diffraction data collection statistics

X-ray diffraction data processing	
Space group	$P3_121$
a, *c*, Å	110.2, 343.1
α, γ, deg	90, 120
Resolution, Å	2.6
Number of unique reflections	70267
Completeness of data, %	93.52
$I/\sigma(I)$	2.643
Rmrgd-F, %	18.8

Crystallization

Crystals of TthPRPPS1 HB27, which were used to collect the X-ray diffraction data set, were grown by the hanging-drop vapor-diffusion method (Fig. 1) from a protein solution with a concentration of 12.3 mg/mL. The protein solution was composed of 20 mM Tris, pH 8.5, 1 mM ATP, 1 mM $MgCl_2$, 5% glycerol, and 0.04% NaN_3. The composition of the reservoir solution was as follows: 5% PEG 1500, 0.45 M KCl, 0.1 M citric acid, pH 5.0, 5 mM $MgCl_2$, and 0.04% NaN_3. The crystals reached the maximum size within one week. Before X-ray diffraction data collection, the crystals were transferred to a cryoprotectant solution composed of 20% glycerol, 5% PEG 1500, 0.45 M KCl, 0.1 M citric acid, pH 5.0, 5 mM $MgCl_2$, and 0.04% NaN_3 and were flash-frozen in liquid nitrogen stream.

X-Ray Diffraction Data Collection and Processing

The X-ray diffraction data set was collected to 2.6 Å resolution from one crystal at 100 K on the European Synchrotron Radiation Facility (ESRF, France, ID23-1 beamline) equipped with the Pilatus6MF detector at a wavelength of 0.96772 Å. The X-ray diffraction data were measured using the rotation method with an oscillation angle of 0.1° and a rotation angle of 360°; the crystal-to-detector distance was 400 mm. The X-ray diffraction data were processed with the iMosflm program [17]. The X-ray diffraction data collection and processing statistics are given in Table 1. The crystals belong to sp. gr. $P3_121$. There are six subunits of the hexameric enzyme molecule per asymmetric unit.

RESULTS AND DISCUSSION

The thermophilic phosphoribosylpyrophosphate synthetases from *Thermus thermophilus* HB27, Tth PRPPS1 and Tth PRPPS2, belong to class 1 phosphoribosylpyrophosphate synthetases. They have a homohexameric quaternary structure and their activity is regulated not only in the active site but also in the allosteric site [14]. Procedures were developed for the isolation of the thermophilic phosphoribosylpyrophosphate synthetases Tth PRPPS1 and Tth PRPPS2, and the enzyme activity was found to depend on the concentrations of metal ions and inorganic phosphate and on the temperature [14]. The synthetases Tth PRPPS1 and Tth PRPPS2 differ in the primary structure and properties [14], although the sequences of these two proteins have a high homology, being somewhat different in the polypeptide chain length. The polypeptide chains of Tth PRPPS1 and Tth PRPPS2 contain 307 and 310 residues, respectively; 152 residues are identical in both sequences; the degree of identity is 48.875% (Fig. 2).

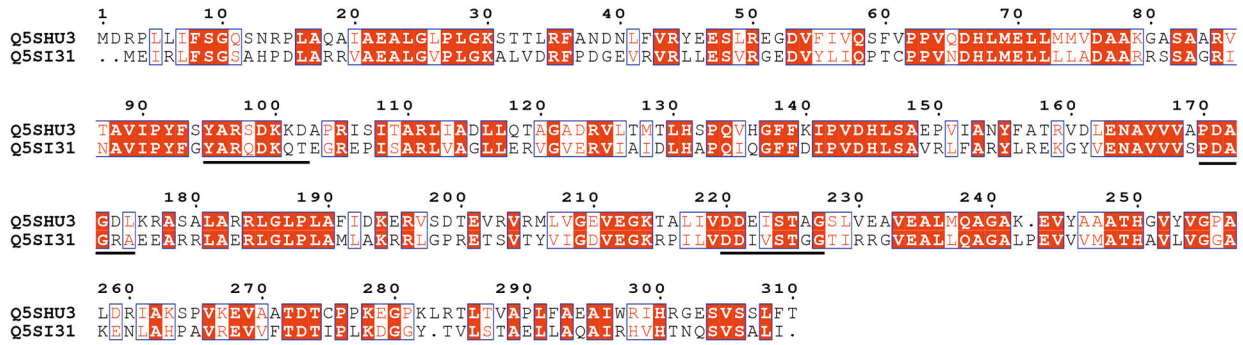

Fig. 2. Sequence alignment of the enzymes Tth PRPPS2 (Q5SHU3) and Tth PRPPS1 (Q5SI31). The catalytically important regions of the enzyme molecule are underlined in black.

Previously, several polypeptide chain segments, which are essential for the function of PRPP synthetase, were identified. They are mainly located in the following flexible regions of the polypeptide chain: the pyrophosphate-binding loop (loop PP_I, residues 170–175; hereinafter, the residue numbers correspond to those in the sequence of Tth PRPPS2), the ribose-5-phosphate-binding loop (loop R5P, residues 220–227), and the flexible loop (residues 95–102) [18, 19]. In class I PRPP synthetases, the active site is located in the cleft between the N- and C-terminal domains. In the N-terminal domain, the active site is bound by the flexible-loop residues; in the C-terminal domain, by the residues of the loops PP_I and R5P. The flexible-loop residues are involved in the binding of the ATP substrate in the active site and of the ADP inhibitor in the regulatory site of the adjacent subunit. The residues of the loop R5P interact with the phosphate ion (sulfate in Tth PRPPS2; PDB_ID: 7AWO). The catalytic loop involves residues necessary for the catalytic activity of the enzyme.

The sequence alignment of the enzymes Tth PRPPS2 and Tth PRPPS1 (Fig. 2) demonstrated that all four segments essential for the function of PRPP synthetase have different residue sequences. The residues are generally divided into groups according to the hydrophobicity or hydrophilicity of their side chains and their charges. Following this classification, most of the differences in the sequences of the four essential segments of Tth PRPPS2 and Tth PRPPS1 are related to residues bearing hydrophobic uncharged side chains. For example, the following substitutions are observed: Ile to Val, Ala to Gly, Ile to Leu, Phe to Met, Pro to Gly, and Leu to Ala. Besides, there are other differences. In the loop R5P and the catalytic flexible loop, the residues Glu222 (the loop R5P) and Asp193, Asp199 (the catalytic loop) with negatively charged side chains in Tth PRPPS2 are replaced by residues with hydrophobic uncharged side chains in Tth PRPPS1 (Glu222, Asp193, and Asp199 by Ile220, Ala191, and Pro197, respectively). In the flexible loop 95–104 of Tth PRPPS2, Ala103 is replaced by Glu101 (Tth PRPPS1) with a charged side chain. In the catalytic loops of the enzymes under consideration, there are replacements of residues bearing hydrophilic uncharged side chains by residues with charged side chains. For example, the residue Thr200 (Tth PRPPS2) is replaced by Arg198 (TthPRPPS1) or the residues Ser201 and Thr203 (Tth PRPPS1) are replaced by Arg203 and Arg205 (Tth PRPPS2).

Two residues of the flexible loop (Arg97 and Lys100 in Tth PRPPS2), which are involved in the substrate binding (ATP) in the active site, are conserved in both sequences. The residues Ser224, Thr225, and Gly227 of the loop R5P, coordinating the sulfate ion in Tth PRPPS2, are also conserved. The conserved residues Asp170 (Asp168 in Tth PRPPS1) of the pyrophosphate-binding loop and Asp220 (Asp218 in Tth PRPPS1) of the ribose-5-phosphate-binding loop are involved in the binding of the metal ion. In the catalytic loops, lysine and arginine residues (Lys194 and Arg196 in Tth PRPPS2; Lys192 and Arg194 in Tth PRPPS1), which are essential for the reaction [13], are also conserved.

It was demonstrated [14] that the enzymes Tth PRPPS1 and Tth PRPPS2 differ in the enzyme activity and the temperature dependence of activity. The enzymes Tth PRPPS1 and Tth PRPPS2 are significantly different in the maximum rate of formation of AMP and phosphoribosylpyrophosphate. At the same temperature (75°C), the rate of the catalysis by Tth PRPPS2 is, on the average, 26 times higher compared to that observed for Tth PRPPS1. The enzyme activity of Tth PRPPS1 significantly increases with increasing temperature. The maximum rate of the enzymatic reaction is observed at 75°C. The activity of Tth PRPPS2 also increases with temperature, reaching the maximum value at 85°C (16 times higher compared to that at 36°C), and then decreases by almost twice at 92°C [14].

The enzyme Tth PRPPS2, characterized by a high temperature of maximum activity, contains a large number of alanine residues (43 residues, 13.9%), which is typical, as it was demonstrated in [20], of pro-

teins from thermophilic organisms. The synthetases Tth PRPPS1 and Tth PRPPS2 differ in the number of alanine residues in the polypeptide chain. Thus, the number of alanine residues in Tth PRPPS1 is somewhat smaller (36 residues, 11.7%). For comparison, PRPPSs from the mesophilic *E. coli* and *B. subtilis* strains contain 33 (10.48%) and 28 (8.83%) alanine residues, respectively.

It is known that class I PRPP synthetases are activated by magnesium and phosphate ions. It is assumed that MgATP is the true substrate of the enzyme. Besides, magnesium ions are directly bound to the enzyme in the allosteric site. The binding mechanism of magnesium and phosphate ions was studied for *E. coli* PRPP synthetase [21, 22].

It was demonstrated that the two enzymes show different dependences of the activity on the magnesium ion concentration. The activity of the enzyme Tth PRPPS1 reaches the maximum value at a magnesium ion concentration of 0.5 mM. A further increase in the magnesium ion concentration leads to a decrease in the activity. The maximum activity of Tth PRPPS1 was observed in the case of a double deficiency of magnesium with respect to ATP. For Tth PRPPS2, the reaction rate significantly increases in the presence of an excess of magnesium, reaching the maximum value at a Mg^{2+} concentration of 5 mM [14].

The investigation of the dependence of the activity of Tth PRPPS1 and Tth PRPPS2 on the phosphate concentration also revealed significant differences between the two proteins [14]. The enzyme Tth PRPPS2 showed the maximum activity at a phosphate concentration of 20 mM, and then the activity of the enzyme was inhibited by an excess of phosphate. The maximum activity of Tth PRPPS1 was observed at a phosphate concentration of 100 mM.

Therefore, both enzymes, Tth PRPPS1 and Tth PRPPS2, belong to class I phosphoribosylpyrophosphate synthetases and are characterized by a high temperature of maximum activity. The determination of the three-dimensional structure of the enzyme will make it possible to reveal the distinguishing structural features of the Tth PRPPS1 molecule.

CONFLICT OF INTEREST

The authors declare no conflicts of interest, financial or otherwise.

FUNDING

The study was supported by the Russian Science Foundation (project no. 21-13-00429) and the Ministry of Science and Higher Education of the Russian Federation within the framework of the state assignment for the Federal Scientific Research Centre "Crystallography and Photonics" of the Russian Academy of Sciences (X-ray diffraction data collection).

REFERENCES

1. R. L. Switzer, J. Biol. Chem. **244**, 2854 (1969).
2. M. A. Becker, K. O. Raivio, B. Bakay, et al., J. Clin. Invest. **65**, 109 (1980).
3. H. G. Khorana, J. F. Fernandes, and A. Kornberg, J. Biol. Chem. **230**, 941 (1958).
4. B. Hove-Jensen, J. Bacteriol. **170**, 1148 (1988).
5. B. Hove-Jensen, Mol. Microbiol. **3**, 1487 (1989).
6. B. Hove-Jensen and P. Nygaard, Eur. J. Biochem. **126**, 327 (1982).
7. B. N. Krath and B. Hove-Jensen, Protein Sci. **10**, 2317 (2001).
8. S. Li, Y. Lu, B. Peng, and J. Ding, Biochem. J. **401**, 39 (2007).
9. A. Kadziola, C. H. Jepsen, E. Johansson, et al., J. Mol. Biol. **354**, 815 (2005).
10. M. M. Cherney, L. T. Cherney, C. R. Garen, and M. N. James, J. Mol. Biol. **413**, 844 (2011).
11. M. Willemoes, B. Hove-Jensen, and S. Larsen, J. Biol. Chem. **275**, 35408 (2000).
12. I. Hilden, B. Hove-Jensen, and K. W. Harlow, J. Biol. Chem. **270**, 20730 (1995).
13. B. Hove-Jensen, A. K. Bentsen, and K. W. Harlow, FEBS J. **272**, 3631 (2005).
14. R. S. Esipov, Yu. A. Abramchik, I. V. Fateev, et al., Bioorg. Khim. **42** (5), 567 (2016).
15. Yu. Abramchik, E. Zayats, M. Kostromina, et al., Crystals **11**, 1128 (2021). https://doi.org/10.3390/cryst11091128
16. V. I. Timofeev, E. V. Sinitsyna, M. A. Kostromina, et al., Acta Crystallogr. F **73**, 369 (2017).
17. T. G. Battye, L. Kontogiannis, O. Johnson, et al., Acta Crystallogr. D **67** (4), 271 (2011). https://doi.org/10.1107/S0907444910048675
18. T. A. Eriksen, A. Kadziola, A. K. Bentsen, et al., Nat. Struct. Biol. **7**, 303 (2000).
19. J. L. Smith, Curr. Opin. Struct. Biol. **5**, 752 (1995).
20. B. Hove-Jensen and J. N. McGuire, Eur. J. Biochem. **271**, 4526 (2004).
21. M. M. Cherney, L. T. Cherney, C. R. Garen, and M. N. James, J. Mol. Biol. **413**, 844 (2011).
22. M. Willemoes and B. Hove-Jensen, Biochemistry **36**, 5078 (1997).

Translated by T. Safonova